Genipin Suppresses Growth and Metastasis in Hepatocellular Carcinoma Through Blocking Activation of STAT-3

Ming Hong (hongming1986@gzucm.edu.cn)
Guangzhou University of Chinese Medicine
Selena Lee
university of kansas
Jacob Clayton
university of kansas
Wildman Yake
university of kansas
Jinke Li
university of kansas

Research

Keywords: Hepatocellular carcinoma, Signal transducer and activator of transcription-3, Genipin, Angiogenesis, Cancer invasion

Posted Date: June 5th, 2020

DOI: https://doi.org/10.21203/rs.3.rs-32717/v1

Version of Record: A version of this preprint was published on August 2nd, 2020. See the published version at https://doi.org/10.1186/s13046-020-01654-3.

Abstract

Background Signal transducer and activator of transcription-3 (STAT-3) can facilitate cancer progression and metastasis by being constitutively active via various signalling. Abundant evidence has indicated that STAT-3 may be a promising molecular target for cancer treatment.

Methods In this study, a dual-luciferase assay-based screening of 537 compounds for STAT-3 inhibitors of hepatocellular carcinoma (HCC) cells was conducted, leading to the identification of genipin. Effects of genipin on HCC were assessed in patient-derived xenograft mice model. Western blotting assay, chromatin immunoprecipitation (ChIP) assay, molecular docking study, tube formation assay, three-dimensional top culture assay, histological examination and immunofluorescence were utilized to evaluate the regulatory signalling pathway.

Results Our research have demonstrated that genipin suppresses STAT-3 phosphorylation and nuclear translocation, which may attribute to the binding capacity of this compound to the Src homology-2 (SH2) domain of STAT-3. In addition, we also demonstrated the therapeutic effects of genipin in patient-derived HCC xenograft mice model.

Conclusion In conclusion, genipin showed therapeutic potential for HCC treatment by interacting with SH2-STAT-3 domain and suppressing the activity of STAT-3. In future study, further research are expected for exploring the potential role of genipin in combination with chemotherapy or radiotherapy for HCC.

Backgroud

Signal transducer and activator of transcription–3 (STAT–3) was originally identified as a critical mediator of IL–6-type cytokine signal pathway and described as an acute phase response factor (APRF) [1, 2], which can operate as a transcription factor of various cytokines, interferons, hormones and growth factors [3]. After dimerization, STAT–3 can transfer to the nucleus and act as transcription activator. Phosphorylation of tyrosine 705 residue induced by epidermal growth factor (EGF) or interleukins can activate STAT–3 in cells [4]. STAT–3 can facilitate cancer progression and metastasis by being constitutively active via various signaling as previously described [5, 6]. Abundant evidences have indicated that STAT–3 may be a promising molecular target for cancer treatment. Inhibiting of STAT–3 activity can be divided into two categories, such as regulating upstream genes of STAT–3 or directly binding to STAT–3 and suppressing its activity [7]. Although directly targeting of STAT–3 is extremely difficult, several novel targeting agents continuously emerge. For example, Bai et al. recently found a highly selective small-molecule degrader of STAT–3, SD–36, which could suppress lymphoma cells growth and inhibit tumor progression in mice model. In addition, several natural products, such as alantolactone and osthole can suppress the phosphorylation and activation of STAT–3 as well as inhibit tumor progression in breast cancer by directly binding with the SH2 domain of STAT–3 [8, 9]. However, none of these candidate agents have been assessed for their binding affinity to STAT–3. Their selectivity with STAT–3 and other STAT family proteins still needs further exploration.

Hepatocellular carcinoma (HCC) is a highly fatal malignant disease which is the third leading cause of cancer-related deaths in developing countries [10]. Most of the HCC patients were diagnosed at an advanced stage, therefore, these patients have few chance for radical therapy. Although major progress in HCC treatment have been achieved in recent years, HCC patients still have a poor prognosis with high rates of metastasis and postoperative recurrence [11]. Thus, further exploring the underlying molecular mechanisms of HCC and developing highly effective therapies for HCC are urgently needed. Persistent activation of STAT–3 has been found in the majority of HCC patient tissues instead of the para-carcinoma tissue and has been closely associated with poor prognosis [12]. There are increasing studies have shown that STAT–3 plays critical roles in HCC growth and metastasis. Therefore, STAT–3 may be a promising therapeutic target in HCC treatment. Clinical studies have explored the potential benefits of STAT–3-targeted agents either used alone or in combination with chemotherapy in HCC patients. Some of these agents have revealed promising clinical efficacy and safety profile in clinical trails [13].

In this study, a dual-luciferase assay-based screening of 537 compounds for STAT–3 inhibitors was conducted, leading to the identification of genipin. Further research have demonstrated that genipin suppresses STAT–3 phosphorylation and nuclear translocation, which may attribute to the binding capacity of this compound to the SH2 domain of STAT–3. Furthermore, we also evaluated the therapeutic effects of genipin in patient-derived HCC xenograft mice model.

Materials And Methods

Cell lines

MHCC97L, HepG2 and LO2 cells were obtained from the American Type Culture Collection (Manassas, VA). The cells were cultured in RPMI 1640 medium containing 10 % FBS at 37 °C in a humidified atmosphere containing 4% CO_2. Media were supplemented with antibiotics including 150 μg/ml of streptomycin and 50 U/ml of penicillin.

Luciferase reporter assay

The luciferase reporter system was applied using the pGMSTAT-3-Luc plasmid for detecting the activation of STAT-3. The plasmid was purchased from GeneTech (Beijing, PRC) and transfected into cells following the instructions in previous study [14]. Before plasmid transfection, MHCC97L cells were cultured in 12-wells plate for 12 hour. Co-transfection of pRL-SV40 (Renilla luciferase) and pGMSTAT-3-Luc was conducted by Lipofectamine 3000 (Thermo Scientific, USA) in MHCC97L cells. 1 day after transfection, MHCC97L cells were exposed to the test chemicals from our internal chemicals library for 12 hour. Luciferase signal was analyzed using the dual-luciferase reporter systems as previously described [15]. The activation of STAT-3 regulated by candidate agents was analyzed by the proportion between the value of Renilla and firefly luciferase activity.

Immunoblotting

Immunoblotting assay was conducted as previously described [16]. The nuclear and cytosol protein were extracted by the Nuclear Protein Extraction kit (Fermentas, USA). The related primary antibodies and secondary antibodies were purchased from Abcam (Cambridge, USA). Antibodies were diluted prior to use following the manufacturer's recommendations.

Real-Time PCR

Total RNA was isolated using TRIzol (Sigma, USA) following the instructions of the manufacturer. The purified RNA was then reverse-transcribed to cDNA with Invitrogen SuperScript IV kit. Real-time PCR experiments were conducted by SYBR Green PCR Kit (QIAGEN, China) reactions were performed for 40 cycles in standard mode using Bio-Rad CFX96 PCR System. The primers used in this study were shown in Supplementary table 3. Each reaction was performed in triplicate.

Cell Viability Assay

Cell viability was examined by using the 3-(4,5-dimethylthiazol-2-yl)-5-(3-carboxymethoxyphenyl)-2-(4-sulfophenyl)-2H-tetrazolium (MTS) assay as previously described [3]. Absorbance was recorded at 490 nm using a Bio-rad PR-4100 microplate reader (Hercules, USA). Each reaction was performed in triplicate.

Immunofluorescent staining

Immunofluorescence staining was performed refer to previous studies [17]. Briefly, after fixation with 4% paraformaldehyde, cells were blocked and hybridizated with the indicated primary antibodies for 12 h. Next, fluorescein isothiocyanate (FITC)-conjugated secondary antibodies were added and incubated for 2 h, 4',6-diamidino-2-phenylindole (DAPI) was used for nuclear staining. The fluorescent expressions of the target marker and nucleus were visualized by confocal microscope (Olympus, Japan).

Electrophoretic mobility shift assay

Electrophoretic mobility shift assay (EMSA) was conducted to evaluate the DNA-binding activity of STAT-3 in genipin treated HCC cells. In brief, following transfection of HCC cells for 72 h, nuclear proteins from each sample were extracted with Nuclear Extraction kit (Sigma, USA) and subjected to EMSA following the manufacturer's standard protocol using the LightShift® Chemiluminescent EMSA kit (Thermo Fisher Scientific, USA). The STAT-3 target probe was synthesized with a 3'-biotin modification (Invitrogen, USA) and the sequence was 5'-ACG AAC CAT TACGCTCGA CAG CCG-3', in which the binding region is underlined. was conducted with STAT-3 EMSA Kit (Thermo Fisher Scientific, USA) following the

instructions of manufacturer. STAT-3 oligonucleotides with infrared dye-label were as follows: 5'-CTACGGACGTACGAACTGCACGGC-3' and 3'-ACCTGGACTAACGTCAGCCGCG-5'.

Chromatin immunoprecipitation (ChIP) assay

HCC cells were added into formaldehyde for immobilizing protein–DNA complex. Then, cell lysis solution was added. DNA fragment was broken by ultrasound. The related antibodies and beads were added to precipitate the protein–DNA complex. The protein–DNA complex was immunoprecipitated with STAT-3 antibody. protein A/G agarose beads were applied to incubate with the immunoprecipitate. Next, the samples were washed by PBS, the chromatin–protein complex was reversed. Phenol-chloroform was used to purify the DNA. Then, DNA sequences were validated by qPCR assay. The primers used in ChIP assay were specific for stat-3-binding sites in the promoters of VEGF, SOCS3, and BCL-2.

Molecular docking study

The three-dimensional structure of STAT-3 were obtained from the RSCB Protein Data Bank(http://www.pdb.org/) (PDB code: 6NJS) and prepared with Sybyl-X 2.0 (Tripos, St. Louis, MO, USA) for the docking studies [18]. An energy minimized 3D structure of Genipin (PubChem: 442424) was optimized from NCBI-PubChem (https://pubchem.ncbi.nlm.nih.gov/). The elaborate docking method and reliability validated assay were recorded in the protocol of Surflex-Dock module of Sybyl-X[19].

Surface Plasmon Resonance (SPR) assay

SPR assay was applied to further validate the binding affinity of genipin with STAT-3-SH2 protein. SPR binding assay was performed with Biocore T300 biosensor systems (General Electric, USA) as previously described [20]. All the SPR-based materials were obtained from General Electric Co. The related target proteins were acquired from R&D systems (Minneapolis, USA). Biocore trace was baseline subtracted and the signals were presented in sensorgram and determined in RU. Empirically in the BIOcore technology, 2 ng of analyte bound at the surface gave a response of 1×10^3 RU. Equilibrium constants (KD) were calculated with the 'affinity' model in Biocore T300 evaluation software version 3.2.

Tube formation assay

HCC cells were plated in a 6-well plate to 95% confluence after 36 hours, then, cells were washed with PBS and the medium was substituted by serum-free medium with different concentration of genipin. Conditioned media were collected after centrifugation at 1200 rpm for 10 min. A total of 2×10^4 HUVECs were seeded into each well of a 12-wells plate coated with 200 µl Matrigel (Sigma, USA), and cultured for 8 hours in conditioned medium. Images were captured by an Olympus CKX41 inverted microscope (magnification ×100; Olympus Corp.), and analyzed for the extent of tube formation by

measuring the tube length and counting the number of tube nodes using the ImageJ software. Each reaction was performed in triplicate.

Immunohistochemistry assay

Immunohistochemical staining was performed according to previous studies[21]. Antibodies for p-STAT-3 and CD31 were provided by Invitrogen (Carlsbad, CA, USA). Immunohistochemistry assay was performed in an automated system using the Ventana® BenchMark Ultra following the manufacturer's protocols. The immunohistochemistry slides were examined by three independent researchers. Positivity for p-STAT-3 and CD31 were defined as unequivocally nuclear and cytoplasmic staining of at least 75% of the cancer cells.

Three-dimensional top culture assay

Growth factor-reduced Matrigel was thawed at 4°C for 12 h. Matrigel solution (60 μL/well) was added into 24-well plates in 35°C for 20 minutes. A total of 2×10^5 MHCC97L cells were resuspended in 150 μL serum-free medium and cultured on solidified Matrigel. 15 minutes post cells attachment, 150 μL serum-free media with 15% Matrigel and indicated concentrations of genipin was added on top of the plated culture. All experiments were repeated by three independent researchers.

Animal studies

For constructing HCC xenograft mice models, BALB/C mice (4 week, female) were orthotopically implanted with 2×10^5 MHCC97L cells refer to our previous studies [18]. 0.2 ml solution of 25 mg/kg ketamine and 15 mg/kg xylazine were used to anesthetize mice by intramuscular injection. 2 weeks later, BALB/C mice were randomly divided into DMSO group (n = 8), 25 mg/kg/day genipin treatment group (n = 8) and 50 mg/kg/day genipin treatment group(n = 8) by i.p. injection. 35 days after treatment, mice were sacrificed and dissected. The liver tumor weight and lung metastasis nodules were measured by three independent researchers. All animal studies were approved and under the strict supervision by the Committee of Experimental Animal Ethics, in the University of Kansas (Approval number: CF201900239).

For the patient-derived xenograft (PDX) model, HCC cells were collected for constructing xenograft model as previously described [10]. Seven surgical liver samples were obtained from HCC patients in the department of hepatobiliary surgery, The first affiliated hospital of Guangzhou University of Chinese medicine (Supplementary table 3). The tumor tissue was incised into small pieces (0.3 cm^3). 75% ethanol was used for surgical disinfection. For anesthesia of mice, 0.6% lidocaine was applied in our study. For establishing the F1 generation, 1 piece of the human HCC tissue was sent into the subcutaneous. When the tumor volume grew to 1 cm^3, the tumor was dissected into two pieces. One piece of tumor was fixed in 4% formaldehyde solution and the other piece was further incised into small pieces (0.3 cm^3). Eight

Balb/c mice were transplanted with tumor tissue as described above (F2 generation). The PDX mice model of F3 generation was also conducted as described above. Then, the mice were randomly divided into DMSO group (n = 8), 25 mg/kg/day genipin treatment group (n = 8) and 50 mg/kg/day genipin treatment group(n = 8) by i.p. injection. Tumor volumes were measured at the indicated time points. All procedures and protocols were approved by the Ethical Committee of The first affiliated hospital of Guangzhou University of Chinese medicine.

Statistical analysis

All data were presented as mean ± SD of three independent experiments. The statistical analyses were evaluated by GraphPad Prism using Student's t-test for comparing two means. ANOVA followed by Tukey's post hoc test was applied for the statistical analysis when more than two means were compared. P values less than 0.05 were considered statistically significant.

Results

Genipin can inhibit the phosphorylation of STAT-3 (Tyr) and decrease the expression of STAT-3 target gene in HCC cells

As a transcription factor, STAT-3 can regulate cell proliferation and angiogenesis through modulating its down-stream target genes such as Bcl-2, VEGF and SOCS-3[22]. To screen novel STAT-3 inhibitory agents, the STAT-3 luciferase reporter system was applied to screen target agents from our internal chemicals library(Fig 1a. up panel). We screened 537 compounds and eventually identified genipin as a novel natural agent for inhibiting STAT-3 signal pathway. Genipin exhibited significant STAT-3 suppressive activity in MHCC97L and HepG2 cells (Fig 1a. down panel). While phosphorylated Y705 has been widely acknowledged to be essential for STAT-3's transcriptional activity; the function of phosphorylated S727 still controversial, as this modification has been reported to have both up- and downregulatory effects on STAT3's transcriptional activity. Thus, for validating the STAT-3 suppressive effects, p-STAT-3 (Y705) and p-STAT-3 (S727) expression were examined by western blot after genipin treatment. Our results showed that genipin (20 μM) remarkably inhibited the activation of pSTAT-3 (Y705) but failed to affect the protein expression of STAT-3 and p-STAT-3 (S727) (Fig 1b). Cytoplasmic STAT-3 exported to the nucleus is a critical step for regulating its down-stream genes expression. Both immunofluorescent staining and western blotting results confirmed that genipin inhibited nuclear translocation of STAT-3 (Fig 1c). Furthermore, STAT-3 DNA-binding ability was inhibited by genipin treatment according to the electrophoretic mobility shift assay results (Fig 1d). Protein tyrosine phosphatases (PTPases) are a group of enzymes that are able to eliminate the DNA binding of STAT-3 [23], thus, we intended to explore whether genipin could inhibit STAT-3 by PTPases in HCC. PTEN, SHP1 and SHP2 are key regulatory PTPases in STAT-3 signal transduction pathways [24], however, the protein expression of these PTPases has no obvious changes after genipin treatment(supplementary Fig 1a). In addition, to further confirm whether genipin inhibits STAT-3 specifically, we also evaluated the activity of STAT-5, STAT-1, STAT-2,

mTOR and MAPK signal pathways by western blotting. Our results indicated that genipin failed to affect the phosphorylation of STAT-5, STAT-1 and STAT-2 as well as the expression of the related proteins in mTOR and MAPK signal pathways (supplementary Fig 1b,c). Up to present, we could conclude that genipin suppressed STAT-3 phosphorylation and nuclear translocation as well as inhibited its DNA-binding ability. STAT-3 dimers exported to the nucleus can activate the promoter of STAT-3 target genes and up-regulates the protein expression of these tumor-related genes such as Survivin, Bcl-2, MMPs, SOCS3 and VEGF [17]. Western blot assay results further confirmed that genipin treatment decreased the expression of STAT-3 target genes in HCC cells (Fig 1e). In addition, chromatin immunoprecipitation assay indicated that genipin inhibited the binding affinity of STAT-3 with Bcl-2, SOCS3 and VEGF(Fig 1f). In summary, above data revealed that genipin could inhibit STAT-3 phosphorylation(Y705) and suppress its target genes expression in liver cancer .

Genipin binds to the SH2 domain in STAT-3

Next, we explored whether genipin could directly interact with STAT-3 by *in silico* assay. As shown in Fig 3a, genipin was docked nicely into the SH2 domain of STAT-3(PDB Id: 1GB1). PHE716, LYS626, GLN635, SER636, GLU638, ARG609, LYS591, VAL637,PRO639 and TRP623 of STAT-3 formed strong interactions with genipin. To further confirm whether genipin can directly bind to STAT-3-SH2 domain, GST-tagged STAT-3-SH2 domain (42kD) was purified from *E.coli* (Fig 2b). Then, surface plasmon resonance (SPR) assay was performed to determine the binding affinity between genipin and STAT-3-SH2. SPR analysis results indicated that STAT-3-SH2 bound to genipin with a relative low dissociation constant (KD) value (KD = 2.3 μM) (Fig 2c). The activation of STAT-3 required phosphorylation on tyrosine and forming a dimer via phosphotyrosine/SH2 domain interaction[25]. Our results showed that genipin distinctly suppressed the interaction between purified STAT-3-SH2 and STAT-3 by GST pull-down assay (Fig 2d). Next, Flag-tagged and HA-tagged STAT-3 vectors were constructed and transfected into MHCC97L cells for validating whether genipin inhibits the dimerization of STAT-3. Our results suggested that HA-STAT-3 co-immunoprecipitated with Flag-STAT-3 in MHCC97L cells and genipin blocked the interplay dose-dependently (Fig 2e). In addition, genipin also inhibited STAT-1: STAT-3 heterodimers formation (Supplementary Fig 2a).These results indicated that genipin might directly bind to the STAT-3-SH2 domain, and inhibit the dimerization of STAT-3 or STAT-1: STAT-3. EGFR can also bind to STAT-3-SH2 domain and activate STAT-3[26]. GST pull-down results indicated that purified STAT-3-SH2 interplayed with EGFR and genipin exposure (20 μM) suppressed the complex formation (Fig 2f). Then, we further explored whether genipin could induce the dissociation of EGFR-STAT-3 complex. We found that treatment with EGF can increase the binding ability of STAT-3 to EGFR in HCC cells while treatment with genipin significantly suppressed these interactions (Fig 2g). These results demonstrated that genipin directly bound with STAT-3-SH2 domain.

Genipin inhibits HCC cells proliferation and angiogenesis *in vitro*

Above results clearly demonstrated that genipin can inhibit STAT-3 activation. To evaluate the anticancer effect of genipin, we examined its potential suppressive effect on HCC cells proliferation by MTS assay. To our surprise, genipin remarkably inhibited HepG2 and MHCC97L cells viability dose-dependently. But, no significant inhibition effect on normal liver cells LO2 was observed in our study(Fig 3a). Western blotting results showed that the phospho-STAT-3 (Tyr-705) level was decreased after genipin treatment in HCC cells but kept unchanged in normal liver cells (LO2) (Supplementary Fig 3a). Next, we further explored whether STAT-3 inhibition is related with impaired cancer cells proliferation. STAT-3 vectors were transfected into MHCC97L cells, overexpression of STAT-3 obviously reversed genipin-mediated tumor growth inhibition and STAT-3 target genes suppression (Fig 3b). Furthermore, genipin (10 μM) could induce apoptotic cell death in HCC cells as indicated by western blotting and Annexin V/7AAD assay (Fig 3c). Then, we further determined whether genipin inhibited colony formation in MHCC97L and HepG2 cells. As shown in Fig 3d, genipin suppressed colony formation in MHCC97L and HepG2 cells in a dose-dependent manner. Accumulating evidence suggests that STAT-3 plays a critical role in angiogenesis under both pathological and physiological conditions in addition to cell proliferation and survival [27]. It has been widely recognized that angiogenesis plays a pivotal role in cancer development as malignant tumor need sufficient blood provision if the tumor is to grow beyond a few cubic millimeters in volume [28]. One of the most widely applied *in vitro* experiments to model the reorganization stage of angiogenesis is the tube construction assay. In our study, genipin failed to affect HUVECs viability (Supplementary Fig 4a) or capillary-like structure construction (Supplementary Fig 4b) in culture medium. However, less well-formed capillary-like structures were built for HUVECs in the MHCC97L-conditioned medium after genipin (10, 20 μM) treatment (Fig 3e). In conclusion, above results revealed that genipin might inhibit HCC proliferation and angiogenesis.

Genipin suppresses HCC cells invasion and reverses the EMT process

The spread and metastasis of cancer cells may occur via invading the surrounding tissues and intravasating into blood or lymphatic circulation through the endothelium [29]. Herein, cell invasion ability was analysed by Transwell assay using MHCC97L and HepG2 cells. Our results showed that genipin (10 μM) inhibited HCC cells invasion dose-dependently (Fig 4a). Cancer invasion requires extracellular matrix (ECM) and basement membrane degradation. Thus, fluorescent-gelatin degradation assay was applied to examine whether genipin suppresses ECM degradation by HCC cells. Our results suggested that MHCC97L cells significantly promoted ECM degradation in control group, while genipin (20, 50 μM) treatment reversed ECM degradation by HCC cells (Fig 4b). Three-dimensional (3D) culture is an artificially created environment which provides functional and structural aspects of cancer development. In this study, our 3D culture results showed that genipin (20, 50 μM) remarkably suppressed HCC cells invasion via the surrounding Matrigel (Fig 4c). Epithelial–mesenchymal transition (EMT) is a key process in cancer metastasis by which epithelial cells lose their polarity and cell-cell adhesion, and obtain invasive and migratory properties. During the EMT process, the expression of several epithelial and

mesenchymal biomarkers significantly changed. Interestingly, genipin treatment notably decreased the expression of vimentin, fibronectin and N-cadherin while increased the expression of E-cadherin in HCC cells (Fig 4d).

Genipin suppresses cancer progression in HCC xenograft tumor models

For further exploring whether genipin suppresses HCC progression *in vivo*, we established orthotopic mice xenograft models with MHCC97L cells. Then, DMSO (0.1%) (vehicle) or genipin were administrated daily by intraperitoneal injection. Fig 5a showed that genipin treatment (25, 50 mg/kg) notably decreased tumor weight, which indicated that genipin could inhibit HCC progression *in vivo*. In addition, genipin treatment also significantly decreased the number of metastasis nodules in lung (Fig 5b, c). Further studies demonstrated that genipin suppressed the protein expression of phospho-STAT-3 (Y705) and inhibited the expressions of STAT-3 target genes in primary liver tumor tissues (Fig 5d, e). Furthermore, decreased vascular density were detected by CD31 stanning in HCC tissues in genipin-treated mice (Fig 5e). The survival rate of mice was analysed for evaluating whether the metastasis inhibition effects of genipin could improve the overall survival rate. Our results showed that genipin significantly improve the survival rate of tumor-bearing mice. No mice was survival in vehicle group (n=8) on day 40, whereas six mice were survival on day 40 and day 50 after genipin (50 mg/kg) treatment (Fig 5f). In conclusion, above results suggested that genipin could inhibit HCC metastasis and improve the overall survival rate in orthotopic transplantation HCC mice models.

Anti-HCC effect of genipin in a patient-derived HCC xenograft mice model

Patient-derived xenograft (PDX) mice model may keep more similarities to the human cancers compared to normal cell-lines xenograft mice model. Previous studies have shown that PDX mice model may be useful for screening novel anti-cancer agents [30]. Herein, seven human surgical HCC tissue samples along with the peripheral normal liver tissues were collected from primary HCC patients (supplementary table 1). Firstly, we detected the protein expressions of STAT-3 and p-STAT-3 (Y705) in these surgical samples. Our results indicated that the expressions of STAT-3 and p-STAT-3 (Y705) were notably reduced in HCC peripheral normal liver tissues compared to tumor tissues (Fig 6a). These results suggested that the activation of STAT-3 is up-regulated in tumor cells derived from HCC patient. After establishing the PDX mice model, we examined the protein expression of STAT-3 and p-STAT-3 (Y705) in tumor-bearing mice. No obvious changes have been found in the expression of p-STAT-3 (Y705) in F0, F1, F2 and F3 passages (Fig 6b). Above results indicated that the activity of STAT-3 has not been changed in patient-derived HCC xenograft mice after serial passages culture. The F3 passages mice were divided into DMSO (0.1%) and genipin (25, 50 mg/kg/day) treatment groups(n=8). After genipin treatment, the HCC growth in mice was significantly suppressed (Fig 6c). The tumor volume in genipin treatment (25, 50 mg/kg/day)

group was 597.43 and 401.26 cubic millimeters, respectively. In contrast, the tumor volume in vehicle treatment group was 1452.24 cubic millimeters (Fig 6d). In addition, Tumor weight in liver remarkably decreased after genipin (25, 50 mg/kg/day) treatment (Fig 6e). Interestingly, genipin also decreased the protein levels of p-STAT-3 (Y705) and STAT-3 target genes (Bcl-2, VEGF, Survivin) in mice model (Fig 6f). immunohistochemistry assay further confirmed the decreased expression of p-STAT-3 (Y705) as well as the tumor vascular density (CD 31+) in HCC samples from PDX mice after administration with genipin (25, 50 mg/kg/day) (Fig 6g).

Genipin inhibits the proliferation of other cancer cells

Considering that STAT-3 signaling regulate oncogenic pathway in various tumor cells, we hypothesized that genipin might also inhibit other cancer cells growth. Fig 7a showed that genipin (20, 50 μM) exposure resulted in the growth inhibition of various kinds of cancer cells . In addition, genipin notably suppressed STAT-3 signal pathway in these tumor cells. Fig. 7b showed that the activation of p-STAT-3(Y705) was significantly inhibited by genipin treatment in various non-HCC cancers.

The potential toxicity of genipin on tumor-bearing mice

For evaluating the potential toxicity of genipin *in vivo*, we further examined the effects of genipin on kidney and liver functions in tumor-bearing mice. No obvious changes on serum creatinine, blood urea nitrogen, aspartate transaminase (AST) and alanine transaminase (ALT) levels between genipin and DMSO group have been detected ($p > 0.05$) (Supplementary Table 2). In addition, body weight changes in mice were detected every 7 days. No significant loss of body weight has been detected after genipin treatment (Supplementary Fig 5a). Furthermore, H&E staining results indicated no obvious histological changes between genipin-treated mice and control mice (Supplementary Fig 5b). In conclusion, these data suggested that genipin exhibit no significant adverse effects on mice at the therapeutic dosage.

Discussion

Discovering novel agents from natural products for HCC treatment may provide promising therapeutic drugs for improving patients survival [31, 32]. In the current study, we found a small natural compound, genipin, could inhibit STAT-3 activity *in vitro* and *in vivo*. Our molecular docking study indicated that genipin could bind to SH2-STAT-3 domain, which was further confirmed by *in vitro* studies. For the first time, we demonstrated that genipin could inhibit HCC progression by targeting STAT-3 signal pathway (Fig.8).

The SH2 domain is a structurally conserved protein domain contained within the STAT-3 protein. SH2 domains can promote STAT-3 dimerization by docking to phosphorylated tyrosine residues on STAT-3[33]. This dimerization changes the STAT-3 conformation and facilities target DNA recognition as well as regulates gene expression. Our *in silico* studies suggested that genipin could bind to SH2-STAT-3 domain.

Which was further confirmed by SPR study. In addition, co-immunoprecipitation assay indicated that genipin inhibited STAT-1:STAT-3 heterodimerization and STAT-3:STAT-3 homodimerization. In previous research, Mahalapbutr, P et. al found that SH2 domain was critical for EGFR and STAT-3 interaction and subsequent STAT-3:STAT-3 homodimerization [34]. In our study, we revealed that genipin could suppress EGFR-STAT-3 interaction and further inhibit STAT-3 dimerization. The STAT-3 has two critical phosphorylation sites, Ser727 and Tyr705, for its activation. However, genipin failed to phosphorylated STAT-3 on Ser727 site in this study. Thus, we speculate that genipin can inhibit STAT-3 activity by suppress STAT-3 phosphorylation on Tyr-705 site.

In this study, genipin suppressed HCC cells proliferation by regulating the expression of survivin, Mcl-1, and Bcl-2 genes. However, genipin failed to affect several common signal pathways which have a close association with cancer proliferation. Such as the mTOR, STAT-5, STAT-1, STAT-2 and MAPK pathways. Thus, we speculated that genipin might inhibit HCC cells proliferation by specifically suppression STAT-3 activity. Ulaganathan, V. K. et. al. have revealed that STAT-3 was constitutively activated in malignancy instead of normal tissues [35, 36]. Interestingly, our results showed that genipin selectively suppressed HCC cells proliferation without significant toxicity in normal cells. These findings suggested that STAT-3 might be a promising therapeutic target for cancer treatment with few side-effects. Vascular endothelial growth factor (VEGF), originally known as vascular permeability factor (VPF), is a signal protein which can stimulate the formation of blood vessels in cancer development [37]. Sim, D. Y. et.al. showed that STAT-3 could regulate the expression of VEGF in various types of cancers [38]. Herein, our results demonstrated that genipin remarkably decreased the expression of VEGF in HCC cells. Chromatin immunoprecipitation results confirmed that STAT-3 could regulate the expression of VEGF and inhibited STAT-3 binding to the promoter region of VEGF. In addition, HUVEC tube construction assay showed that less well-formed capillary-like structures were built for HUVECs in the tumor-conditioned medium derived from genipin treated cells. *In vivo* studies further confirmed the decreased cancer vascular density in mice after genipin treatment by IHC assay. As a conclusion, the decreased expression of VEGF regulated by STAT-3 might contribute to genipin-induced cancer angiogenesis suppression.

Cancer metastasis is a pathological process which malignant cells spread from a primary site to a different site within the host's body [39, 40]. The degradation of ECM plays a pivotal role in the process of metastasis. MMP-2, a type IV collagenase can facilitate ECM degradation and promote cancer metastasis. Previous studies have shown that STAT-3 could regulate the expression of MMP-2 in cancer cells[41]. In our study, genipin notably suppressed the expression of MMP-2 in HCC cells and inhibit the degradation of ECM. The epithelial–mesenchymal transition (EMT) is a process by which epithelial cell lose polarity and adhesion ability, which can promote cancer cells metastasis [42]. Xiong, H. et.al. found that STAT-3 might directly induce EMT progression and modulate ZEB1 expression in colon cancer cells. Knockdown of STAT-3 can up-regulate the expressions of E-cadherin and down-regulate N-cadherin and vimentin in colon cancer [1]. According to our results, genipin can also regulate EMT-relevant proteins expression in HCC. Furthermore, genipin treatment remarkably suppressed HCC lung metastasis in xenograft mice model. Above results suggested that genipin might inhibit MMP-2 expression and block the process of EMT in HCC by targeting STAT-3 activity, which could suppress HCC metastasis.

Patient-derived xenograft (PDX) mice model refers to transferring of human cancer samples to immunodeficient mice after surgical operation. As PDX can be passaged without *in vitro* processing procedures, PDX model enable the propagation and expansion of human cancers without oblivious genetic transformation of cancer cells over multiple murine generations [43]. Within PDX model, human cancer can grow in physiologically-relevant cancer microenvironment that mimic the hormone, nutrients and oxygen levels that are observed in the primary human cancer tissues [44]. Thus, PDX model shows significant advantages over established cancer cell lines in cancer research. Herein, we found genipin exhibit notable therapeutic effects in a HCC PDX mice model. Our *in vivo* results indicated that the expression level of p-STAT-3 (Y705) was higher in cancer tissues than para-carcinoma tissues. Furthermore, HCC PDX mice still exhibit high expression of p-STAT-3 (Y705) after continuous passage.

In conclusion, genipin showed therapeutic potential for HCC treatment by directly interacting with SH2-STAT-3 domain, which suppressed the activity of STAT-3. Our study may be the baseline research for future clinical trials and suggests genipin as a novel inhibitor of STAT-3. In addition, more in-depth research could be conducted to explore the potential role of genipin in combination with chemotherapy for HCC in future studies.

Conclusion

In conclusion, genipin showed therapeutic potential for HCC treatment by interacting with SH2-STAT-3 domain and suppressing the activity of STAT-3. In future study, further research are expected for exploring the potential role of genipin in combination with chemotherapy or radiotherapy for HCC.

Abbreviations

PDX: Patient-derived xenograft ; DMSO: Dimethylsulfoxide; HCC: Hepatocellular Carcinoma; STAT-3: Signal Transducers and Activators of Transcription-3; MMP-2: Matrixmetallo proteinase-2; EMT: Epithelial-mesenchymal transition; VEGF: Vascular endothelial growth factor; VPF: originally known as vascular permeability factor; ECM: Extracellular matrix; SPR: Surface plasmon resonance; PTPases: Protein tyrosine phosphatases.

Declaration

Consent for publication

Written informed consent for publication was obtained from all participants.

Availability of data and materials

All the data and materials supporting the conclusions were included in the main paper.

Author Contributions

M.H., S.L., J.C., W.Y., and J.L. performed experiments and analysed the data. M.H.and J.L. designed the experiments. J.L. partially supervised the project. M.H. conceived and supervised the project. M.H. and J.L. cowrote the paper.

Acknowledgments

We thank the Xing-lin Foundation of Guangzhou University of Chinese Medicine for supporting Dr. Ming Hong as a scholar visitor at The University of Kansas. This work was supported by Xing-lin Foundation of Guangzhou University of Chinese Medicine in PRC (GZF-1366732K) and the Funding from National Institutes of Health grants NS79432 in The United States.

Competing interests

The authors declare no competing interests.

Ethics approval and consent to participate

All clinical samples were collected with informed consent from patients, and the study was approved by the Ethics Committee of Guangzhou University of Chinse Medicine, PRC. Animal experiments were carried out in accordance with and under approval of the Experimental Animal Ethics Committee in University of Kansas, USA.

Reference

1. H. Xiong, J. Hong, W. Du, Y.W. Lin, L.L. Ren, Y.C. Wang, W.Y. Su, J.L. Wang, Y. Cui, Z.H. Wang, J.Y. Fang, Roles of STAT3 and ZEB1 proteins in E-cadherin down-regulation and human colorectal cancer epithelial-mesenchymal transition, J Biol Chem, 287 (2012) 5819-5832.
2. C. Weber, Y. Zhou, J.G. Lee, L.L. Looger, G. Qian, C. Ge, B. Capel, Temperature-dependent sex determination is mediated by pSTAT3 repression of Kdm6b, Science, 368 (2020) 303-306.
3. L. Yang, B. Han, M. Zhang, Y.H. Wang, K. Tao, M.X. Zhu, K. He, Z.G. Zhang, S. Hou, Activation of BK Channels Prevents Hepatic Stellate Cell Activation and Liver Fibrosis Through the Suppression of TGFbeta1/SMAD3 and JAK/STAT3 Profibrotic Signaling Pathways, Front Pharmacol, 11 (2020) 165.
4. V. Annamalai, M. Kotakonda, V. Periyannan, JAK1/STAT3 regulatory effect of beta-caryophyllene on MG-63 osteosarcoma cells via ROS-induced apoptotic mitochondrial pathway by DNA fragmentation, J Biochem Mol Toxicol, (2020) e22514.
5. J.J. Balic, M.I. Saad, R. Dawson, A.J. West, L. McLeod, A.C. West, K. D'Costa, V. Deswaerte, A. Dev, W. Sievert, D.J. Gough, P.S. Bhathal, R.L. Ferrero, B.J. Jenkins, Constitutive STAT3 Serine

Phosphorylation Promotes Helicobacter-Mediated Gastric Disease, Am J Pathol, (2020).

6. S. Busker, W. Qian, M. Haraldsson, B. Espinosa, L. Johansson, S. Attarha, I. Kolosenko, J. Liu, M. Dagnell, D. Grander, E.S.J. Arner, K.P. Tamm, B.D.G. Page, Irreversible TrxR1 inhibitors block STAT3 activity and induce cancer cell death, Sci Adv, 6 (2020) eaax7945.
7. M. Cosenza, M. Civallero, L. Marcheselli, S. Sacchi, S. Pozzi, Citarinostat and Momelotinib co-target HDAC6 and JAK2/STAT3 in lymphoid malignant cell lines: a potential new therapeutic combination, Apoptosis, (2020).
8. X. Dai, C. Yin, Y. Zhang, G. Guo, C. Zhao, O. Wang, Y. Xiang, X. Zhang, G. Liang, Osthole inhibits triple negative breast cancer cells by suppressing STAT3, J Exp Clin Cancer Res, 37 (2018) 322.
9. J. Chun, R.J. Li, M.S. Cheng, Y.S. Kim, Alantolactone selectively suppresses STAT3 activation and exhibits potent anticancer activity in MDA-MB-231 cells, Cancer Lett, 357 (2015) 393-403.
10. S. Mancarella, S. Krol, A. Crovace, S. Leporatti, F. Dituri, M. Frusciante, G. Giannelli, Validation of Hepatocellular Carcinoma Experimental Models for TGF-beta Promoting Tumor Progression, Cancers (Basel), 11 (2019).
11. J. Bruix, S. Qin, P. Merle, A. Granito, Y.H. Huang, G. Bodoky, M. Pracht, O. Yokosuka, O. Rosmorduc, V. Breder, R. Gerolami, G. Masi, P.J. Ross, T. Song, J.P. Bronowicki, I. Ollivier-Hourmand, M. Kudo, A.L. Cheng, J.M. Llovet, R.S. Finn, M.A. LeBerre, A. Baumhauer, G. Meinhardt, G. Han, R. Investigators, Regorafenib for patients with hepatocellular carcinoma who progressed on sorafenib treatment (RESORCE): a randomised, double-blind, placebo-controlled, phase 3 trial, Lancet, 389 (2017) 56-66.
12. Y. Ashizawa, S. Kuboki, H. Nojima, H. Yoshitomi, K. Furukawa, T. Takayashiki, S. Takano, M. Miyazaki, M. Ohtsuka, OLFM4 Enhances STAT3 Activation and Promotes Tumor Progression by Inhibiting GRIM19 Expression in Human Hepatocellular Carcinoma, Hepatol Commun, 3 (2019) 954-970.
13. C. Lee, S.T. Cheung, STAT3: An Emerging Therapeutic Target for Hepatocellular Carcinoma, Cancers (Basel), 11 (2019).
14. L. Penolazzi, E. Lambertini, L. Scussel Bergamin, C. Gandini, A. Musio, P. De Bonis, M. Cavallo, R. Piva, Reciprocal Regulation of TRPS1 and miR-221 in Intervertebral Disc Cells, Cells, 8 (2019).
15. M. Hong, J. Li, S. Li, M.M. Almutairi, Resveratrol Derivative, Trans-3, 5, 4'-Trimethoxystilbene, Prevents the Developing of Atherosclerotic Lesions and Attenuates Cholesterol Accumulation in Macrophage Foam Cells, Mol Nutr Food Res, (2020) e1901115.
16. M. Hong, J. Li, S. Li, M.A. M, Acetylshikonin Sensitizes Hepatocellular Carcinoma Cells to Apoptosis through ROS-Mediated Caspase Activation, Cells, 8 (2019).
17. Z.H. Zhang, M.Y. Li, Z. Wang, H.X. Zuo, J.Y. Wang, Y. Xing, C. Jin, G. Xu, L. Piao, H. Piao, J. Ma, X. Jin, Convallatoxin promotes apoptosis and inhibits proliferation and angiogenesis through crosstalk between JAK2/STAT3 (T705) and mTOR/STAT3 (S727) signaling pathways in colorectal cancer, Phytomedicine, 68 (2020) 153172.
18. M. Hong, M.M. Almutairi, S. Li, J. Li, Wogonin inhibits cell cycle progression by activating the glycogen synthase kinase-3 beta in hepatocellular carcinoma, Phytomedicine, 68 (2020) 153174.

19. D. Kumar, S. Shankar, R.K. Srivastava, Rottlerin-induced autophagy leads to the apoptosis in breast cancer stem cells: molecular mechanisms, Mol Cancer, 12 (2013) 171.
20. P.K.R. Kumar, Systematic Screening of Viral Entry Inhibitors Using Surface Plasmon Resonance, Methods Mol Biol, 2089 (2020) 131-145.
21. M.V. Rodriguez, M.A. Sortino, J.J. Ivancovich, J.M. Pellegrino, L.S. Favier, M.P. Raimondi, M.A. Gattuso, S.A. Zacchino, Detection of synergistic combinations of Baccharis extracts with terbinafine against Trichophyton rubrum with high throughput screening synergy assay (HTSS) followed by 3D graphs. Behavior of some of their components, Phytomedicine, 20 (2013) 1230-1239.
22. B. Foglia, S. Sutti, D. Pedicini, S. Cannito, C. Bocca, M. Maggiora, M.R. Bevacqua, C. Rosso, E. Bugianesi, E. Albano, E. Novo, M. Parola, Oncostatin M, A Profibrogenic Mediator Overexpressed in Non-Alcoholic Fatty Liver Disease, Stimulates Migration of Hepatic Myofibroblasts, Cells, 9 (2019).
23. D.E. Cressman, R.H. Diamond, R. Taub, Rapid activation of the Stat3 transcription complex in liver regeneration, Hepatology, 21 (1995) 1443-1449.
24. J. Irie-Sasaki, T. Sasaki, W. Matsumoto, A. Opavsky, M. Cheng, G. Welstead, E. Griffiths, C. Krawczyk, C.D. Richardson, K. Aitken, N. Iscove, G. Koretzky, P. Johnson, P. Liu, D.M. Rothstein, J.M. Penninger, CD45 is a JAK phosphatase and negatively regulates cytokine receptor signalling, Nature, 409 (2001) 349-354.
25. S.H. Baek, J.H. Ko, H. Lee, J. Jung, M. Kong, J.W. Lee, J. Lee, A. Chinnathambi, M.E. Zayed, S.A. Alharbi, S.G. Lee, B.S. Shim, G. Sethi, S.H. Kim, W.M. Yang, J.Y. Um, K.S. Ahn, Resveratrol inhibits STAT3 signaling pathway through the induction of SOCS-1: Role in apoptosis induction and radiosensitization in head and neck tumor cells, Phytomedicine, 23 (2016) 566-577.
26. J. Schueler, C. Tschuch, K. Klingner, D. Bug, A.L. Peille, L. de Koning, E. Oswald, H. Klett, W. Sommergruber, Induction of Acquired Resistance towards EGFR Inhibitor Gefitinib in a Patient-Derived Xenograft Model of Non-Small Cell Lung Cancer and Subsequent Molecular Characterization, Cells, 8 (2019).
27. M. Hong, H. Shi, N. Wang, H.Y. Tan, Q. Wang, Y. Feng, Dual Effects of Chinese Herbal Medicines on Angiogenesis in Cancer and Ischemic Stroke Treatments: Role of HIF-1 Network, Front Pharmacol, 10 (2019) 696.
28. D.H. Ilson, Angiogenesis in gastric cancer: hitting the target?, Lancet, 383 (2014) 4-6.
29. Y.L. Hsu, L.Y. Wu, M.F. Hou, E.M. Tsai, J.N. Lee, H.L. Liang, Y.J. Jong, C.H. Hung, P.L. Kuo, Glabridin, an isoflavan from licorice root, inhibits migration, invasion and angiogenesis of MDA-MB-231 human breast adenocarcinoma cells by inhibiting focal adhesion kinase/Rho signaling pathway, Mol Nutr Food Res, 55 (2011) 318-327.
30. S. Sharma, T. Zhang, W. Michowski, V.W. Rebecca, M. Xiao, R. Ferretti, J.M. Suski, R.T. Bronson, J.A. Paulo, D. Frederick, A. Fassl, G.M. Boland, Y. Geng, J.A. Lees, R.H. Medema, M. Herlyn, S.P. Gygi, P. Sicinski, Targeting the cyclin-dependent kinase 5 in metastatic melanoma, Proc Natl Acad Sci U S A, 117 (2020) 8001-8012.

31. C.W. Tzeng, W.S. Tzeng, L.T. Lin, C.W. Lee, F.L. Yen, C.C. Lin, Enhanced autophagic activity of artocarpin in human hepatocellular carcinoma cells through improving its solubility by a nanoparticle system, Phytomedicine, 23 (2016) 528-540.
32. R. Kant, C.H. Yen, C.K. Lu, Y.C. Lin, J.H. Li, Y.M. Chen, Identification of 1,2,3,4,6-Penta-O-galloyl-beta-d-glucopyranoside as a Glycine N-Methyltransferase Enhancer by High-Throughput Screening of Natural Products Inhibits Hepatocellular Carcinoma, Int J Mol Sci, 17 (2016).
33. W. Zhao, S. Jaganathan, J. Turkson, A cell-permeable Stat3 SH2 domain mimetic inhibits Stat3 activation and induces antitumor cell effects in vitro, J Biol Chem, 285 (2010) 35855-35865.
34. P. Mahalapbutr, P. Wonganan, W. Chavasiri, T. Rungrotmongkol, Butoxy Mansonone G Inhibits STAT3 and Akt Signaling Pathways in Non-Small Cell Lung Cancers: Combined Experimental and Theoretical Investigations, Cancers (Basel), 11 (2019).
35. V.K. Ulaganathan, B. Sperl, U.R. Rapp, A. Ullrich, Germline variant FGFR4 p.G388R exposes a membrane-proximal STAT3 binding site, Nature, 528 (2015) 570-574.
36. A. Di Sotto, S. Di Giacomo, E. Rubini, A. Macone, M. Gulli, C.L. Mammola, M. Eufemi, R. Mancinelli, G. Mazzanti, Modulation of STAT3 Signaling, Cell Redox Defenses and Cell Cycle Checkpoints by beta-Caryophyllene in Cholangiocarcinoma Cells: Possible Mechanisms Accounting for Doxorubicin Chemosensitization and Chemoprevention, Cells, 9 (2020).
37. H. Saman, S.S. Raza, S. Uddin, K. Rasul, Inducing Angiogenesis, a Key Step in Cancer Vascularization, and Treatment Approaches, Cancers (Basel), 12 (2020).
38. D.Y. Sim, H.J. Lee, J.H. Jung, E. Im, J. Hwang, D.S. Kim, S.H. Kim, Suppression of STAT3 Phosphorylation and RelA/p65 Acetylation Mediated by MicroRNA134 Plays a Pivotal Role in the Apoptotic Effect of Lambertianic Acid, Int J Mol Sci, 20 (2019).
39. M. Nakayama, C.P. Hong, H. Oshima, E. Sakai, S.J. Kim, M. Oshima, Loss of wild-type p53 promotes mutant p53-driven metastasis through acquisition of survival and tumor-initiating properties, Nat Commun, 11 (2020) 2333.
40. C.A. Klein, Cancer. The metastasis cascade, Science, 321 (2008) 1785-1787.
41. T. Redmer, Deciphering mechanisms of brain metastasis in melanoma - the gist of the matter, Mol Cancer, 17 (2018) 106.
42. J.R. Rock, C.E. Barkauskas, M.J. Cronce, Y. Xue, J.R. Harris, J. Liang, P.W. Noble, B.L. Hogan, Multiple stromal populations contribute to pulmonary fibrosis without evidence for epithelial to mesenchymal transition, Proc Natl Acad Sci U S A, 108 (2011) E1475-1483.
43. E. Stewart, S.M. Federico, X. Chen, A.A. Shelat, C. Bradley, B. Gordon, A. Karlstrom, N.R. Twarog, M.R. Clay, A. Bahrami, B.B. Freeman, 3rd, B. Xu, X. Zhou, J. Wu, V. Honnell, M. Ocarz, K. Blankenship, J. Dapper, E.R. Mardis, R.K. Wilson, J. Downing, J. Zhang, J. Easton, A. Pappo, M.A. Dyer, Orthotopic patient-derived xenografts of paediatric solid tumours, Nature, 549 (2017) 96-100.
44. Y.A. Evrard, A. Srivastava, J. Randjelovic, N.P. Consortium, J.H. Doroshow, D.A. Dean, J.S. Morris, J.H. Chuang, Systematic Establishment of Robustness and Standards in Patient-Derived Xenograft Experiments and Analysis, Cancer Res, (2020).

Figures

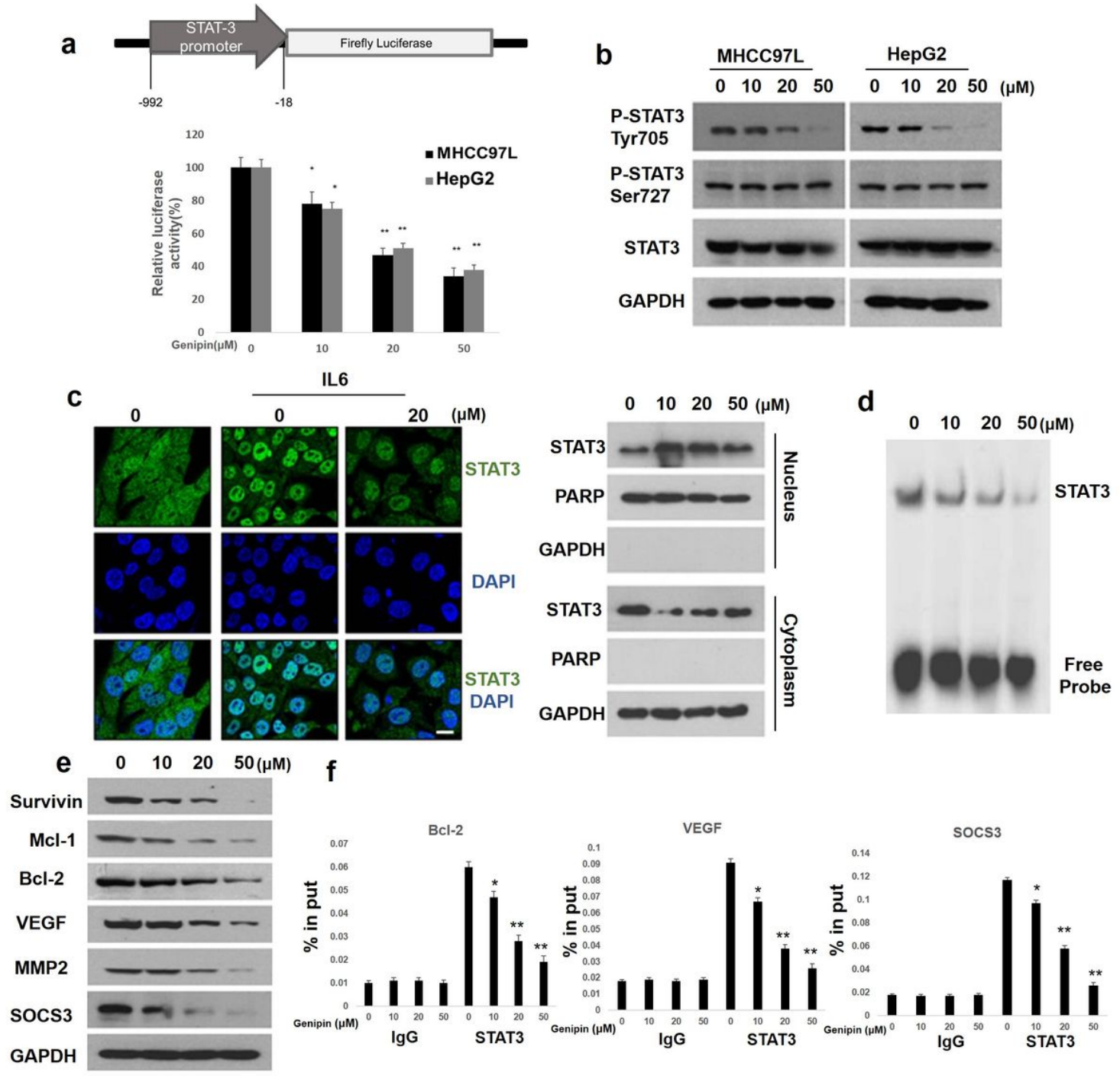

Figure 1

Genipin suppresses STAT-3 activity in HCC. (a) HCC cells were treated with genipin for 24 hour before transfecting with plasmid containing the luciferase reporter gene. The relative luciferase activity was detected using the dual-luciferase reporter systems (b) liver cancer cells were treated with genipin for 24 hour, western blot was performed to detect the protein expression of STAT-3, p-STAT-3 (Y705) and p-STAT-3 (S727). (c) MHCC97L cells were seeded in coverslips coated with gelatin, then genipin(0-20 μM) was added into each samples for 12 hour and co-cultured with or without 10 ng/μl IL-6 for 20 minutes. STAT-3

expression and location was examined by immunofluorescent staining. Cell nuclei were detected by DAPI stanning (Left). MHCC97L cells were seeded in coverslips coated with gelatin, then cells were treated with genipin for 12 hour and co-cultured with or without 10 ng/μl IL-6 for 20 minutes. Cytoplasmic and nuclear STAT-3 levels were detected by western blotting assay(Right) (D) MHCC97L cells were exposed to genipin for 24 hour. STAT-3 DNA-binding activity was analyzed by EMSA assay. (E) MHCC97L cells were exposed to genipin for 24 hour. The protein expression of STAT-3 target genes were examined by western blot assay. (F) MHCC97L cells were exposed to genipin for 24 hour. The binding ability of STAT-3 with its target genes were analyzed by ChIP assay. The data were presented as mean±s.d. *P<0.05; **P<0.01.

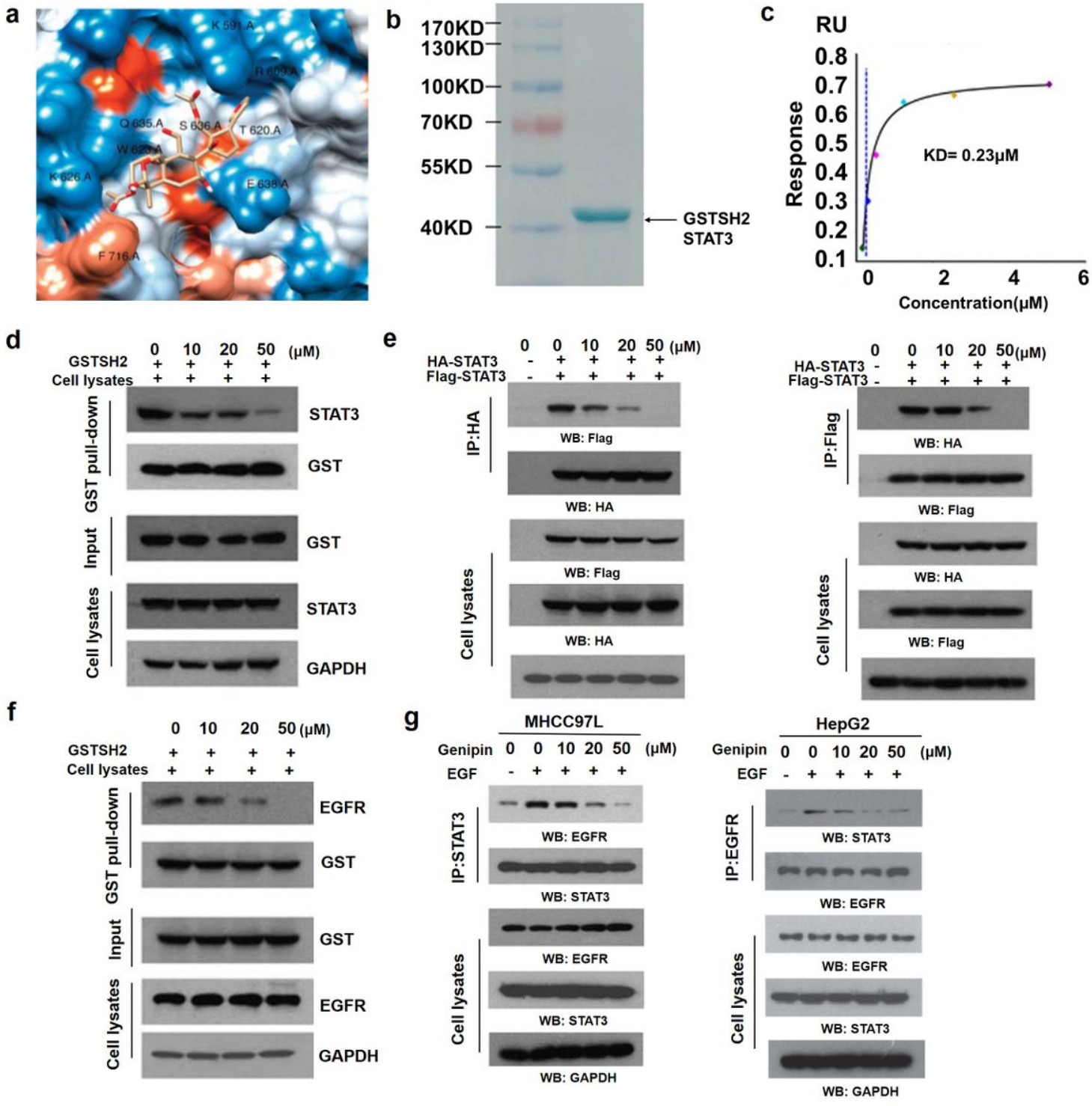

Figure 2

Genipin directly binds with STAT-3-SH2 domain. (a) The three dimensional docking results indicated that genipin could bind to the SH2 domain in STAT-3. (b) The purified GST-tagged STAT-3-SH2 protein was analysed by SDS-PAGE. Coomassie blue was used to stain the target protein. (c) The fitted curve for different concentrations of genipin binding to immobilized STAT-3 by the 'Affinity' model in the Biocore T300 evaluation software. The dot in different colours represent different concentrations of genipin. (d) Genipin suppressed SH2–SH2 interactions. Purified STAT-3-SH2 domain was incubated with MHCC97L cell lysates after mixing with different dosage of genipin for 1.5 h and analysed by GST pull-down assay. (e) Genipin suppressed the dimerization of STAT-3. MHCC97L cells transfected with HA and FLAG -tagged STAT-3 vectors were pre-treated with genipin, the interaction of FLAG-STAT-3 and HA-STAT-3 were validated by immunoprecipitation assay. (f) Purified STAT-3-SH2 domain was incubated with MHCC97L cell lysates after mixing with different dosage of genipin for 1.5 h, the interactions of STAT-3-SH2 with EGFR was validated by GST pull-down. (g) HCC cells (MHCC97L and HepG2) were pre-treated with different dosage of genipin and incubated with EGF, the interactions of STAT-3 with EGFR was validated by co-immunoprecipitation.

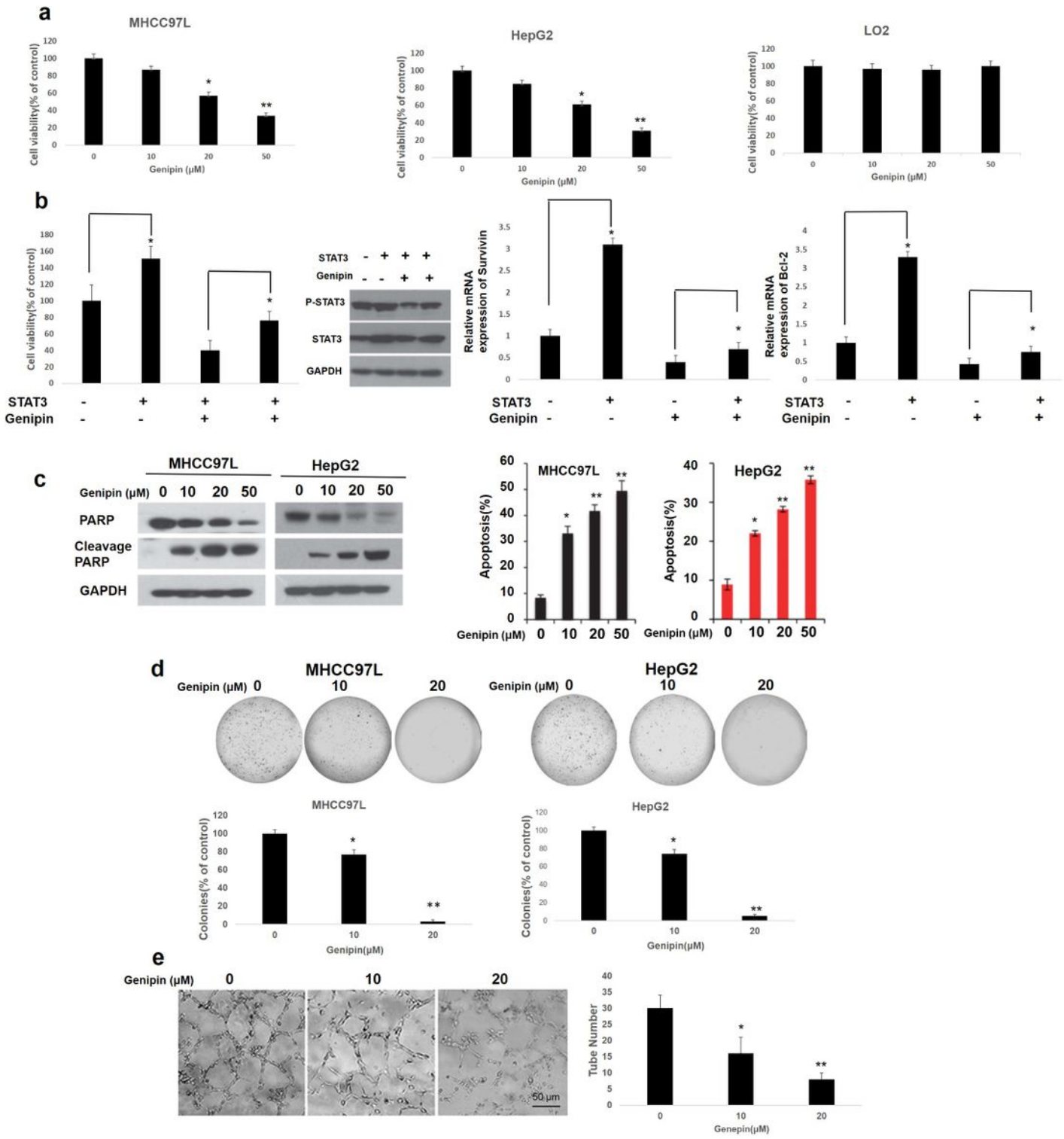

Figure 3

Genipin inhibits HCC cells proliferation and angiogenesis. (a) MHCC97L, HepG2 or normal haptic cells LO2 were treated with different dosages of genipin for 24 hour. Cell viability was detected by MTS assay. (b) STAT-3 vector was transfected into MHCC97L cells. Cell viability was detected by MTS assay, the protein expression of STAT-3 target genes were examined by western blotting. (c) HCC cells were pre-treated with different concentrations of genipin for 24 h, cell apoptosis was analysed by flow cytometry

using Annexin V/7AAD commercial kit. The expressions of PARP and cleaved PARP were examined by western blot assay. (d) Colony formation assays were used to detect HCC cells proliferation ability. MHCC97L and HepG2 cells were incubated with 20 μM genipin for two weeks. Results were shown in the histogram from three independent experiments. (e) Angiogenesis was detected by tube formation assay. 1×105 HUVECs were cultured on Matrigel. Cells were incubated with genipin for 10 hour, representative images of tube formation were observed under an inverted microscope (Leica, Germany) and the relative tube number were analysed. The data were presented as mean±s.d. *P<0.05; **P<0.01

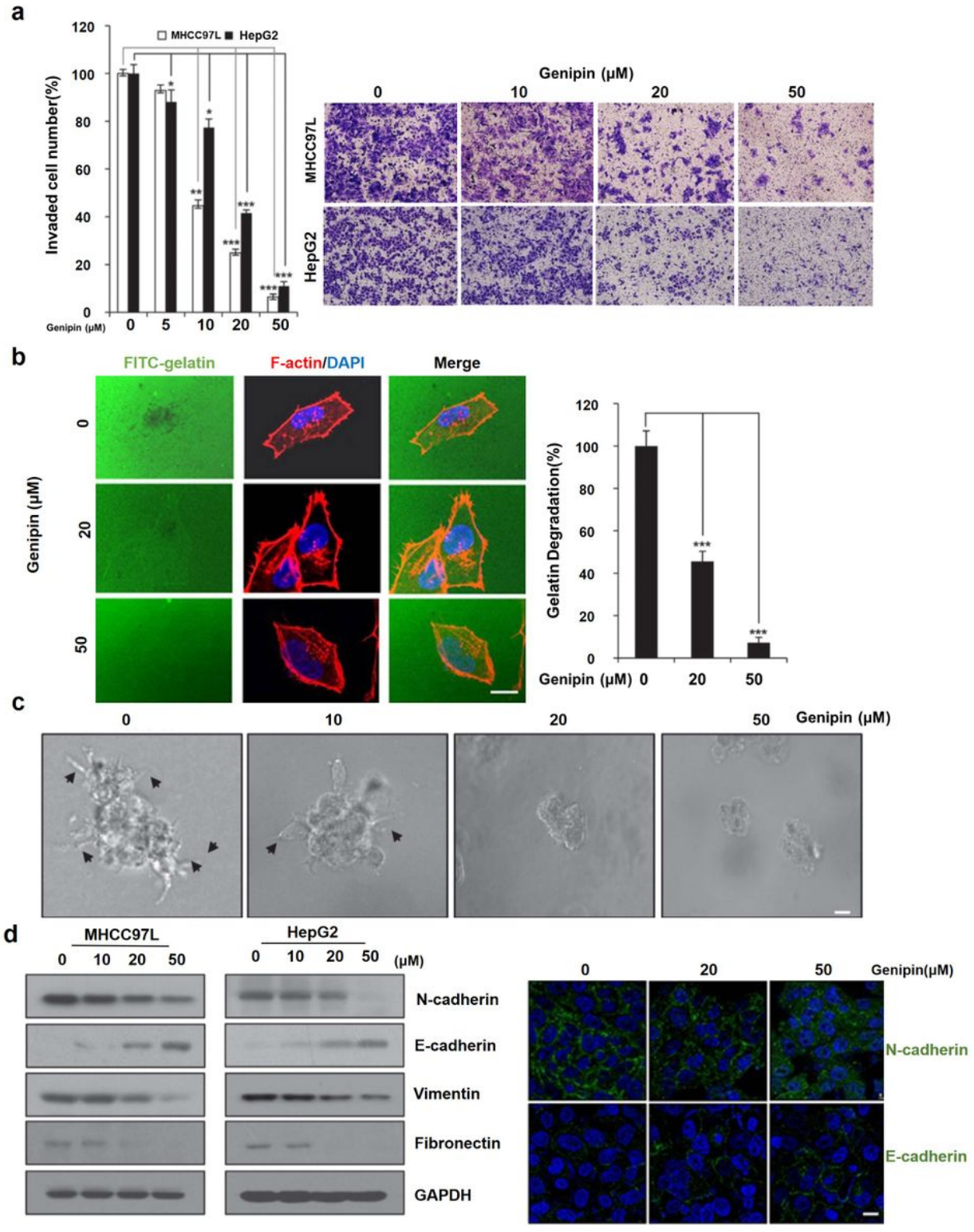

Figure 4

Genipin suppresses HCC cells invasion and reverses EMT process. (a) MHCC97L and HepG2 cells were cultured in the transwell inserts (upper chamber). Images were obtained under optical microscope after genipin treatment 12 h later, invaded cells were calculated by 3 individual researchers. Scale bar = 50 μm. (b) MHCC97L cells were cultured in FITC-conjugated gelatin (green) for 24 h. Phalloidin was applied to stain F-actin (red) and DAPI was used to indicate nuclei (blue). The black area underneath the cell indicated gelatin degradation area, Scale bar = 20 μm. (c) To construct the 3D culture system, MHCC97L cells were seeded into a layer of Matrigel. Then, different dosages of genipin with DMEM and 15% Matrigel was added. The upper mixture was replaced every 24 h. Images were obtained under optical microscope after genipin treatment 96 h later, Scale bar = 50 μm. (d) The protein expression of vimentin, fibronectin, N-cadherin and E-cadherin were validated by western blot and immunofluorescence staining (green). Nuclei was stained by DAPI (blue). Scale bar = 20 μm. Data were presented as mean±s.d, *P<0.05; **P<0.01; ***P<0.001.

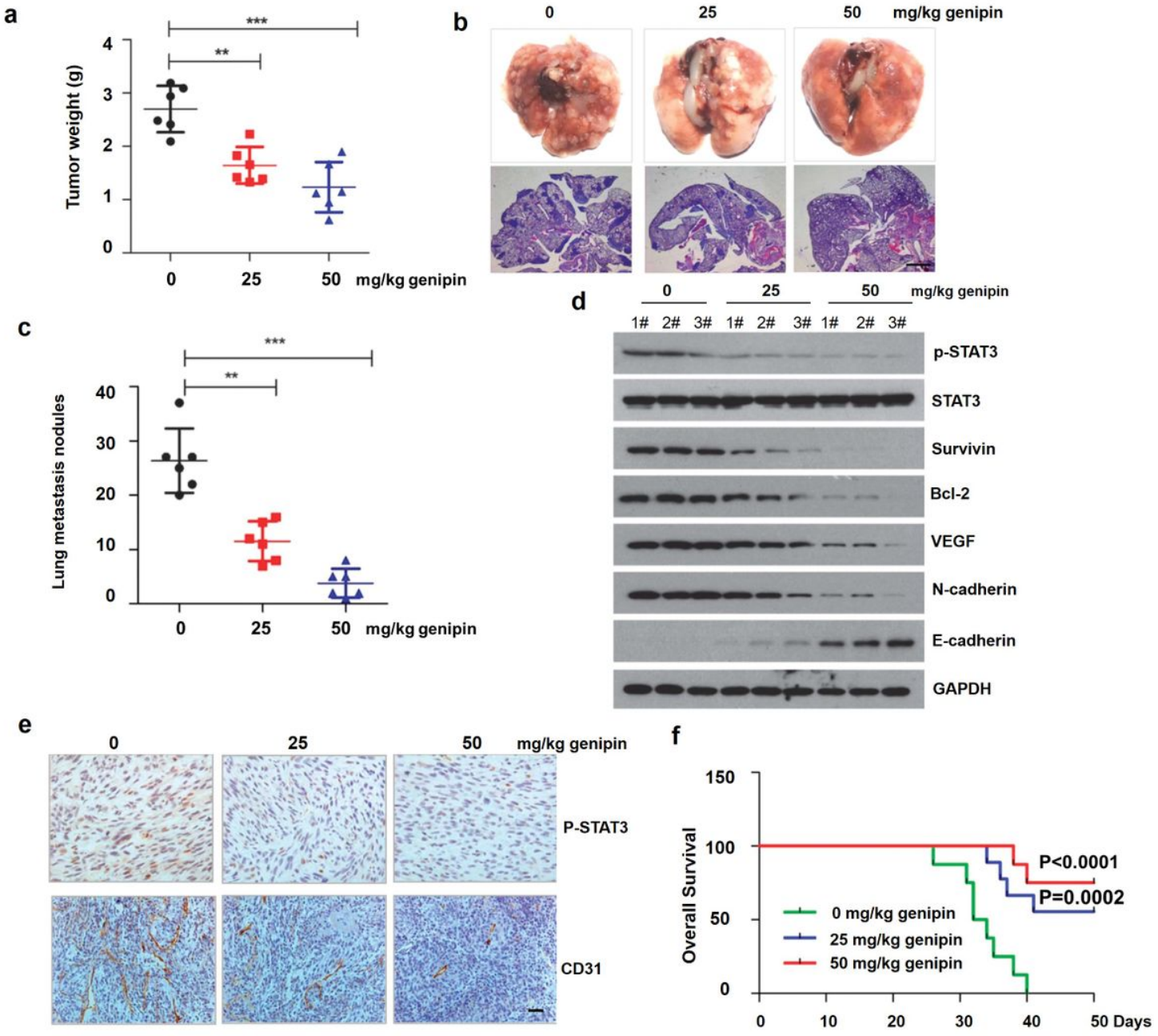

Figure 5

Genipin suppresses HCC progression and improve the survival rate of tumor-bearing mice. MHCC97L cells (5 × 105) were used to established orthotopic mice xenograft models. The tumor-bearing mice were administrated with DSMO or genipin by intraperitoneal injection(n=8). (a) The tumor weight of primary liver cancer in mice was detected after DSMO (0.1%) or genipin treatment. (b) To evaluate lung metastasis in orthotopic transplantation HCC mice, lung tissues were dissected after DSMO or genipin treatment. Representative paraffin sections of lung tissue were stained with hematoxylin and eosin at 20X magnification. Scale bar represents 100 μm. (c) Lung metastasis was examined under anatomic microscope and the number of metastasis nodules was calculated by three individual researchers. (d) The protein expression of p-STAT-3 (Y705) and target genes expression in primary liver tumors were detected by western blot assay. (e) The protein expressions of CD31 and phospho-STAT-3 were evaluated

by immunohistochemical method. Scale bar = 40 μm. (f) Overall survival was analyzed after DSMO or genipin treatment (0-50 days) in tumor-bearing mice. Genipin versus vehicle (25 mg/kg), P=0.0002; Genipin versus vehicle (50 mg/kg), P<0.0001. Data were presented as mean±s.d, **P<0.01; ***P<0.001.

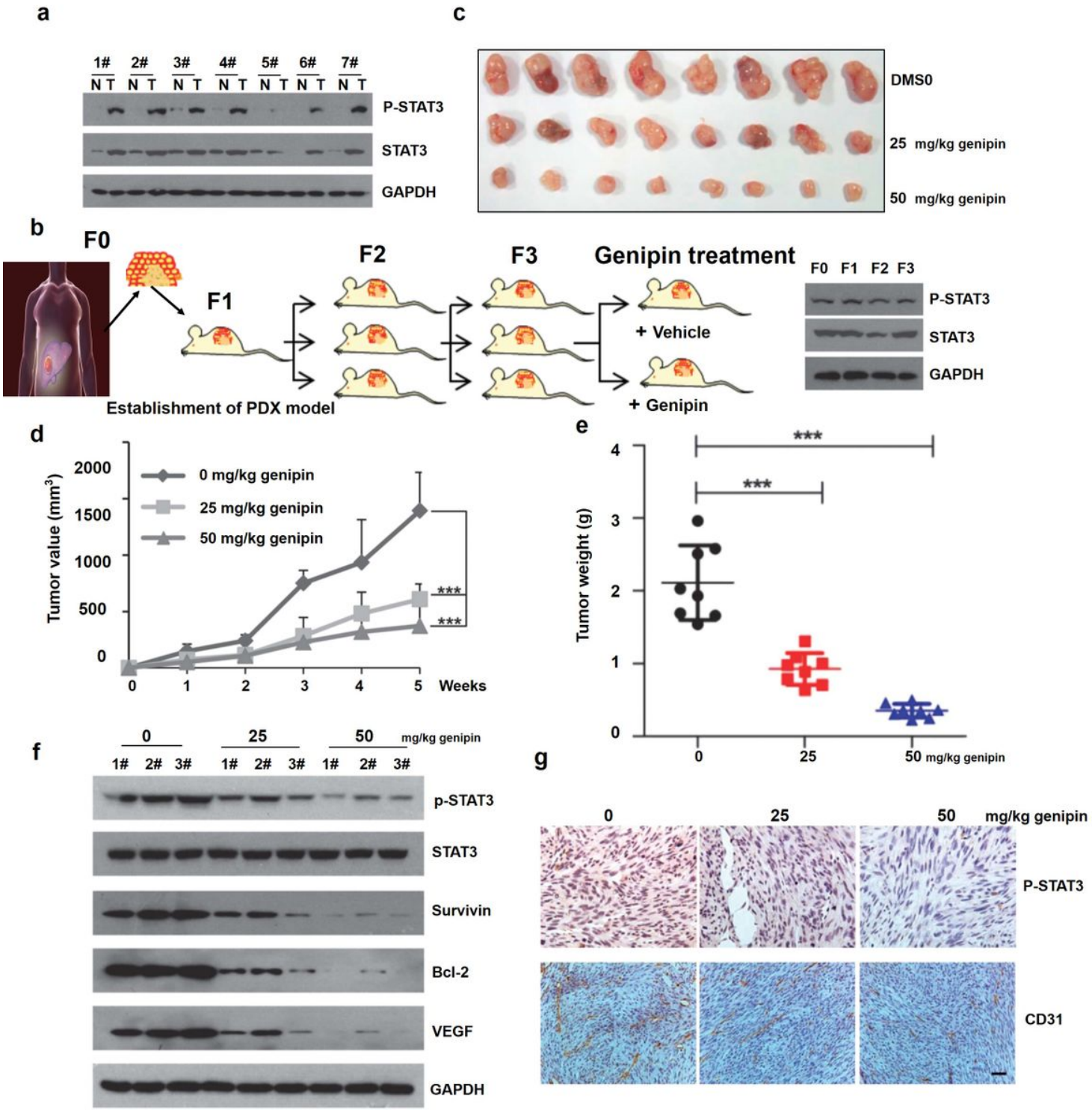

Figure 6

Genipin exhibits anti-HCC effects of in a PDX mice model. (a) The protein expression of STAT-3 and p-STAT-3 (Y705) in human HCC tissue and para-carcinoma tissue were examined by western blot assay. (b) The graphical representation of constructing a PDX mice model. The protein expression of STAT-3 and p-

STAT-3 (Y705) were detected in F1, F2 and F3 generation. (c) Tumor sizes were measured after genipin treatment in PDX model (n=8). (d) The tumor volume in PDX mice was examined after genipin treatment (n=8). (e) The tumor weight in PDX mice was examined after genipin treatment (n=8). (f) The expression of p-STAT-3, STAT-3, Survivin, Bcl-2 and VEGF were examined by western blotting in HCC tissues. (g) The expression of CD31 and p-STAT-3 was validated by immunohistochemistry assay in HCC tissues. Scale bar = 40 μm. Data were presented as mean±s.d, **P<0.01; ***P<0.001.

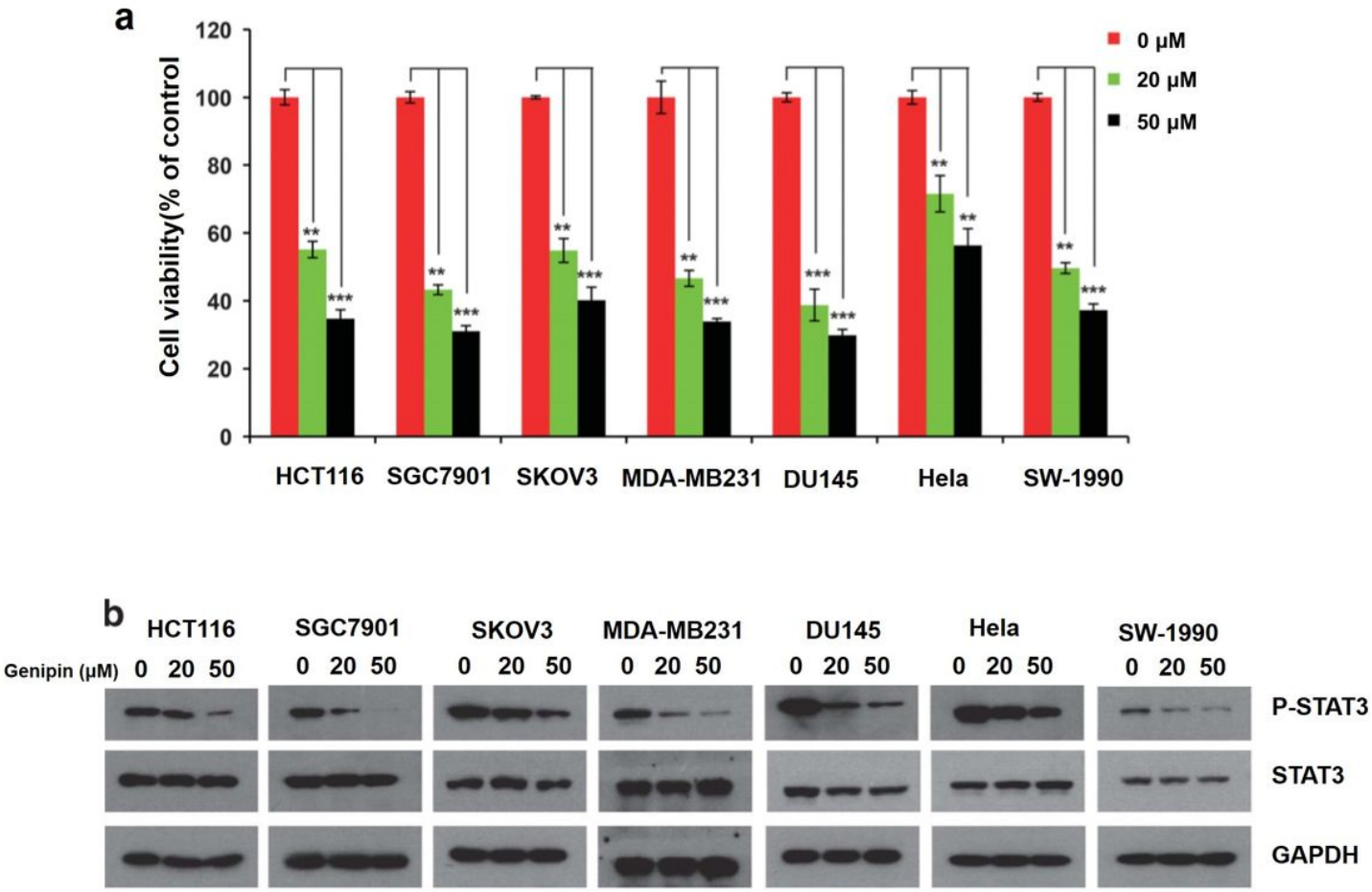

Figure 7

Genipin suppresses the proliferation of various non-HCC cancer cells. (a) Colon, gastric, ovarian, breast, prostate, cervix and pancreas cancer cells were pretreated with genipin (20, 50 μM). Living cells were detected by MTS assay after 36 hour's incubation. (b) various non-HCC cancer cells were pretreated with genipin (20, 50 μM) for 12 hour. The expression of p-STAT-3 and total STAT-3 were examined by western blot assay. Data were presented as mean±s.d, **P<0.01; ***P<0.001.

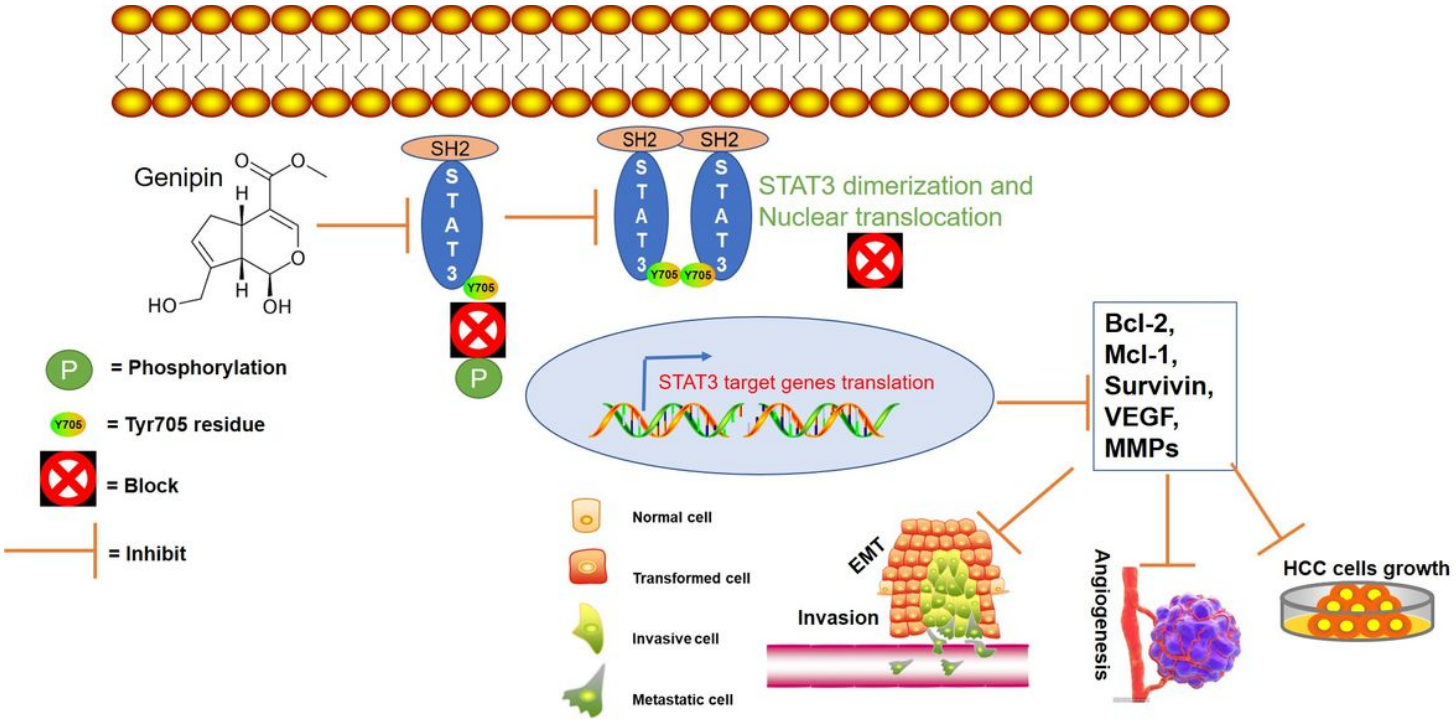

Figure 8

Graphic illustration of the signalling underlying the molecular mechanism of anti-HCC effects of genipin

Supplementary Files

This is a list of supplementary files associated with this preprint. Click to download.

- SUPFIG.docx